Biocompatible 3D Printed Yttria-Stabilized Zirconia parts using Direct Ink Writing

Irene Buj-Corral[1,*], Hector Sanz-Fraile[2], Aitor Tejo-Otero[1], Elena Xuriguera[3], Jorge Otero [2,4]

[1] Department of Mechanical Engineering, School of Engineering of Barcelona (ETSEIB), Universitat Politècnica de Catalunya, Av. Diagonal, 647, 08028 Barcelona, Spain

[2]Unit of Biophysics and Bioengineering. School of Medicine and Health Sciences. Universitat de Barcelona. Barcelona. Spain.

[3] Department of Materials Science and Physical Chemistry, Universitat de Barcelona, Carrer Martí i Franquès 1, 08028 Barcelona, Spain

[4] CIBER de Enfermedades Respiratorias, Madrid, Spain

*Corresponding author: irene.buj@upc.edu

Abstract

Metals such as titanium alloys or Cr-Co alloys have been the most widely used materials in biomedical applications that require high mechanical properties, such as implantology. However, a major disadvantage of these materials is related to the release of ion metals to the body. As an alternative, prostheses made of ceramic materials produce less debris and have better durability. The aim of the present work is to culture human bone-marrow-derived mesenchymal stem cells (hBM-MSCs) on 3D printed rough yttria-stabilized zirconia parts to study their biocompatibility. For that, surface roughness and biocompatibility tests are carried out, and it was confirmed that 3 mol % yttria-stabilized zirconia is a promising material due to its high biocompatibility.

1. Introduction

Metals have been the most widely used materials in biomedical applications that require excellent mechanical properties, such as implantology. However, a major disadvantage of these materials is related to the release of ion metals. These may cause inflammatory and hypersensitivity reactions [1]. Additionally, a failure in medical implants such as hip or knee would lead to the removal of the device and the need to implant a new one. As an alternative, research in the use of ceramics is growing in popularity. Prostheses made from ceramic materials produce less debris and have better durability than those made from metals or plastics [2].

Amongst the different ceramics used in prosthetics (such as hydroxyapatite [3], or alumina [4,5]), zirconia [4] offers several advantages: (1) reduction in the wear rate of implants [6] and the risk of toxicity [7]; (2) excellent biocompatibility [8] and corrosion resistance [9]; (3) outstanding mechanical properties for the manufacture of prostheses [8]. Zirconia has a monoclinic structure at room temperature. As temperature increases, it changes to tetragonal and later to cubic. The transition between monoclinic and tetragonal leads to an important volume change. For this reason, yttria is often added to zirconia to stabilize it with a mix of tetragonal and cubic structures at room temperature [10]. Among the different parameters that can affect the performance of the ceramics is related to their surface roughness, for example in terms of fracture toughness.

One of the most employed AM techniques for ceramics is Direct Ink Writing (DIW), an extrusion technique in which a ceramic paste is extruded and subsequently deposited layer-by-layer[11]. Different ceramic materials can be printed with DIW, for example, kaolinite clay ceramics[12], zirconia[13], zirconia-toughened alumina[14] or hydroxiapatite[15].

Yttria-stabilized zirconia (YSZ) is a biocompatible ceramic with high mechanical properties. It also has the advantage that it can be 3D printed in order to manufacture complex shapes such as prostheses or dental implants [16,17]. Nevertheless, to the author's knowledge, few *in vitro* studies are known for proving the biocompatibility of 3D printed YSZ [18,19]. On the other hand, the surface finish of ceramics is known to affect their mechanical properties [20] and also influence their biocompatibility[21]. In addition, surface roughness is related to bacterial growth in dental implants[22]. The aim of the present research study is to culture human bone-marrow-derived mesenchymal stem cells (hBM-MSCs) on 3D printed yttria-stabilized zirconia parts with different surface roughness values to assess their suitability.

2. Materials and Methods

2.1. Zirconia parts preparation for cell culture

Zirconia pastes were prepared in a mixer. Mixing time was 2 min and rotational speed was 2000 min^{-1}. Vacuum pressure was used to enable both dispersions of materials and removal of bubbles (ARV-310P Thinky Corporation, Tokyo, Japan). Yttria-stabilized zirconia (YSZ) with a 3 mol% concentration (HSY-3B, Daiichi Kigenso Kagaku Kogyo Co., Ltd., Japan) and a 0.5 % wt dispersant (Dolapix PC75, Zschimmer & Schwarz, Germany) were mixed to a Pluronic F-127

(Sigma-Aldrich, UK) stock solution of 25 wt% concentration. The final solid percentage was 40 v%. The d50 value of the ceramic powder ranged between 0.7 and 1.5 µm.

Disk-shaped samples of diameter 10 mm and height 4 mm were printed and subsequently sintered at 1550 °C, with a heating rate of 5 °C/min. The final dimensions of the disks were around 8.5 mm in diameter and 3 mm in height. A linear infill pattern of raster angle 0° was used, with different infill values of 80% and 95% respectively. Three replicates were considered for each experiment.

A customized 3D printer was used, Dual Paste Extruder, from CIM-UPC (Figure 1). Nozzle diameter was 0.58 mm, layer height was 0.3 mm, printing speed was 5 mm/s and the extrusion multiplier was 100%.

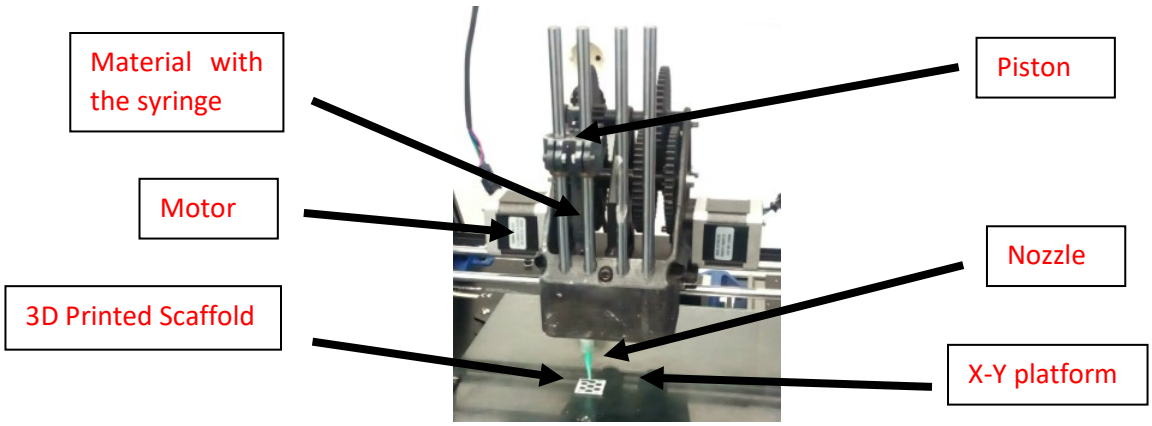

Figure 1. *Printing head of the Dual Paste extruder from CIM-UPC*

2.2. Surface roughness characterization

According to [23], the different roughness parameters can be divided into six groups: (1) amplitude, (2) spatial, (3) hybrid, (4) functional, (5) feature, and (6) other 3D parameters. In the present study, not only areal an arithmetical mean studied, but also skewness (S_{sk}) and kurtosis (S_{ku}). S_a (Equation 1) is the average value of the heights, expressed as an absolute value, regarding the central plane [13]. S_{sk} (Equation 2) corresponds to the symmetry of the heights concerning the central plane. A positive S_{sk} value indicates the predominance of peaks, while a negative value corresponds to the predominance of valleys [24]. Kurtosis parameter S_{ku} (Equation 3) is related to the peakedness of the surface. Sharp peaks and valleys correspond to S_{ku} >3, while rounded peaks and valleys are related to S_{ku} <3 [24]. Both parameters are related to the friction control of surfaces [25].

A Smartproof 5 confocal microscope (Zeiss, Oberkochen, Germany) was used to measure areal roughness, with a 20X magnification lens. Optical equipment was used, to prevent damage to

the samples and/or to the tip of a contact roughness meter [26]. The uncertainty of the microscope in the vertical direction is ± (0.1 µm + 0.008 × L), whereas in the horizontal direction it is ± (0.1 µm + 0.012 × L). Areal parameters were determined according to ISO 25178 standard [27].

$$S_a = \frac{1}{A} \iint_A |Z\ (x,y)|\ dxdy \quad (1)$$

$$S_{ku} = \frac{1}{A_q^4} \iint_A |Z\ (x,y)|^3\ dxdy \quad (2)$$

$$S_{sk} = \frac{1}{A} \iint_A |Z\ (x,y)|\ dxdy \quad (3)$$

where A is the measured area and Z (x, y) is a function that corresponds to the surface topography.

Roughness was measured on the upper surface of the disks, within an area of 0.5 x 0.5 mm.

2.3. BM-MSCs culture

hBM-MSCs are widely used in regenerative medicine and they are a widely accepted model to test the biocompatibility of new scaffold developments [28]. hBM-MSCs were expanded and cultured following the manufacturer's instructions (ATCC, VA). The medium was replaced every 2 days and cells were split from T-75 flasks at reaching 80% confluence. Cells in passage 5 were used for this study. 3D printed zirconia scaffolds were sterilized by high pressure and vapor using an autoclave (Tomy SX-700E) before seeding the cells, and half of them were coated with type I collagen at a concentration of 0.1 mg/mL (Merck, US). Cells were seeded with a density of $4 \cdot 10^4$ cells/cm^2 and cultured for 24h and 72h. At the endpoint, samples were stained for DNA (NucBlue) to identify cell nuclei and imaged with a confocal microscope with a monitored X-Y stage (Nikon TI-HUBC, Japan) with a 10x objective.

3. Results and Discussion

3.1. Surface Roughness

Table 1 shows the average values of areal arithmetic mean, skewness, and kurtosis of both 80% and 95% porosity experiments. Overall, both porosities show a smooth roughness, no sharp or rounded valley or as well as the presence of high peaks or deep valleys. Figure 2 shows the surface topography of the 3D-printed parts.

Table 1. Surface roughness of the upper surface of the yttria-stabilized zirconia samples.

	Sa [µm]	Ssk	Sku
80% porosity	0.30±0.026	-0.002±0.48	10.35±8.37
95% porosity	0.69±0.007	-0.137±0.048	5.03±0.41

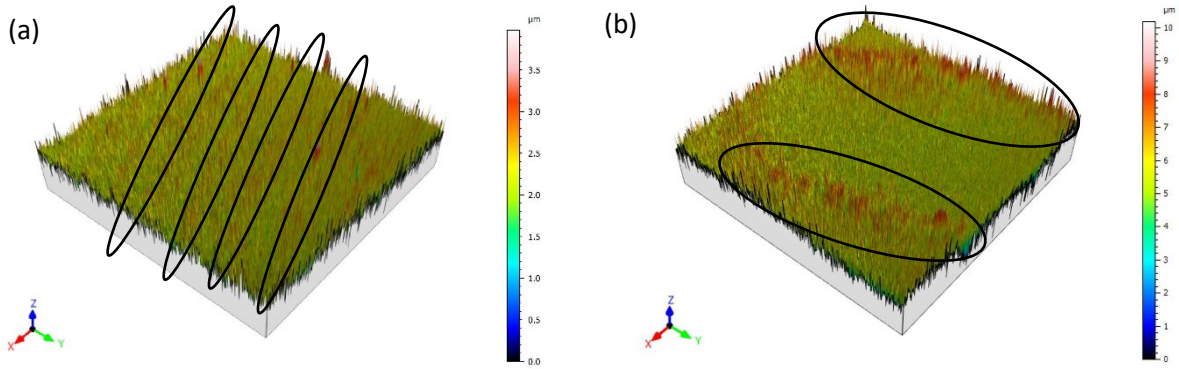

Figure 2. *Surface topography of YSZ parts printed with: (a) 80% infill, (b) 95% infill*

The surface topographies show that the different printed lines were fused, showing no holes among them. In Figure 2a, several parallel crests are observed, corresponding to the deposition of material along parallel lines in the linear structure. In Figure 2b only some crests are observed, showing that, due to an excess of material, the paste has mixed. As for Sa values in Table 1, higher roughness values are observed for 95 % infill (Figure 2b) than for 80 % infill (Figure 2a). This suggests that, for high infill value of 95 % there is an excess of material that leads to higher crests. A slightly negative value for S_{sk} was reported for 95 % infill (Figure 2b), showing higher valleys than peaks. As for S_{ku}, the high value of 10.35 was obtained for 80 % infill, corresponding to sharp peaks and valleys, with a lower value of 5.03 for 95 % infill. In both cases, S_{ku} was higher than 3, which corresponds to a normal distribution of heights.

Shao et al. [29] reported surface roughness close to 8 µm for zirconia. For implants, Sa values below or equal to 1 µm are considered to be smooth, while values above 1 µm are rough [30]. Therefore, the samples in the present study are smooth and, therefore, it is not necessary to undertake a subsequent polishing operation. Additionally, the surface roughness obtained in lateral walls of

yttria-stabilized zirconia pastes depends on print speed. The lower speed, the smoother the surface is [31]. In the present work, however, the roughness was measured on the upper surface of the printed parts to assess its influence on cell compatibility.

3.2. *In vitro* biocompatibility assessment

As can be observed in Figure 3, hBM-MSCs were able to attach to the 3D printed zirconia scaffolds and showed good viability after 3 days of culture (no differences were observed between 24h and 72h of culture). It is noticeable that no differences were observed between uncoated and coated samples (type I collagen), showing that the bare material is biocompatible enough to allow direct cell culture on top without the need for functionalization, so unspecific adhesions formed by MSCs on bare scaffolds are enough for them to proliferate. Collagen has been proven to enhance biocompatibility mainly on metallic substrates such as titanium[32] or magnesium alloys[33] but it might not be so effective on ceramic substrates. On the other hand, although a higher proliferation might be observed in the higher infill scaffolds, the difference is not significant enough to extract conclusions about the most appropriate infill parameter.

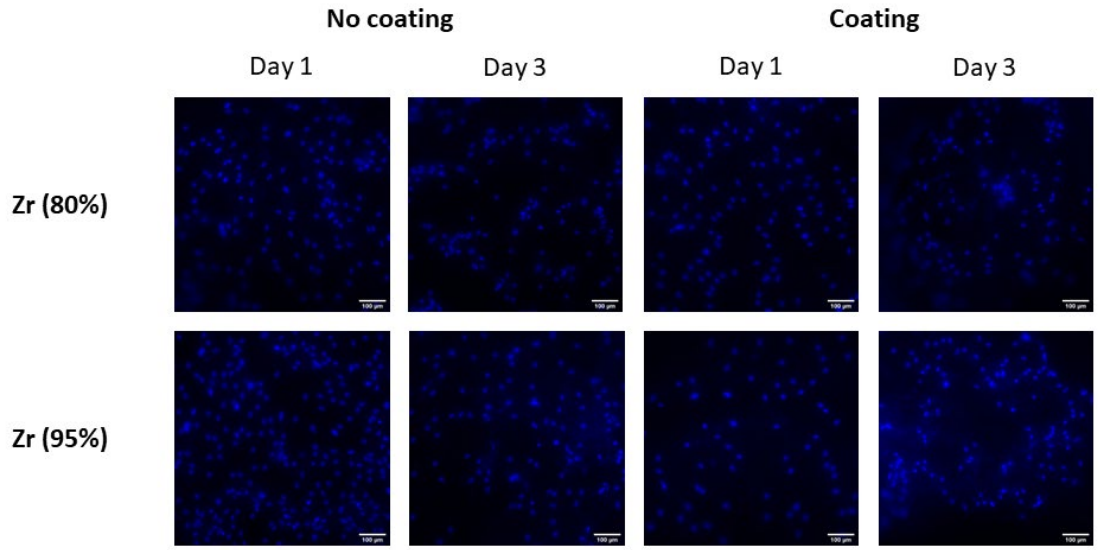

Figure 3. *Fluorescent images (DAPI, cell nuclei) of hBM-MSCs cultured for 24h or 72h on zirconia scaffolds (80% or 95% of porosity) with and without type I collagen coating.*

The surface properties of the scaffolds directly affect cellular behavior. A too smooth or too rough scaffold could cause the cells not to adhere or to modify their behaviour. For example, in soft hydrogels osteodifferentiation increased with surface roughness, being important from Rq values around 0.38 µm, while in stiff hydrogels higher osteodifferentiation was observed for intermediate roughness values[34]. In this work, the areal average roughness Sa measured in the

above scaffolds, between 0.30±.026 µm and 0.69±0.0 µm, led to a good cell proliferation behavior as shown in Figure 3. Thus, it seems that scaffolds' roughness makes them suitable for MSCs culture.

4. Conclusions

In the present work, 3D-printed yttria-stabilized zirconia parts are presented to be used as a novel material in implantology. It was found that the physical properties of the material, such as the surface topography, make the material a suitable candidate for prosthetics. The culture on top of the developed scaffolds of hBM-MSCs showed high viability. Interestingly, there was no difference between bare parts and those coated with an extracellular matrix protein to increase adhesion, so the 3D printed scaffolds could be used without further processing. This opens a door in the field of personalized medicine, as scaffolds could be directly printed with the needed shape before the intervention in the patient. Further research *in vivo*, by implanting the developed scaffolds in animals, would be needed to evaluate the scaffolds presented herein, but *in vitro* results suggest that biocompatibility would not be a limiting factor in those experiments.

Acknowledgments

This work was co-financed by the European Union Regional Development Fund within the framework of the ERDF Operational Program of Catalonia 2014–2020 with a grant of 50% of total cost eligible, project BASE3D, grant number 001-P-001646. Authors would like to thank Alejandro Domínguez and Daniel Vidal for their help with the experimental tests.

References

1. Czarnek K, Terpilowska S, Siwicki AK. Selected aspects of the action of cobalt ions in the human body. *Cent Eur J Immunol* 2015; 40: 236–242.

2. Lerouge S, Huk O, Yahia L, et al. Characterization of in vivo wear debris from ceramic-ceramic total hip arthroplasties. *J Biomed Mater Res* 1996; 32: 627–633.

3. Hamdi DA, Jiang ZT, No K, et al. Biocompatibility study of multi-layered hydroxyapatite coatings synthesized on Ti-6Al-4V alloys by RF magnetron sputtering for prosthetic-orthopaedic implant applications. *Appl Surf Sci* 2019; 463: 292–299.

4. De Aza AH, Chevalier J, Fantozzi G, et al. Crack growth resistance of zirconia toughened alumina ceramics for joint prostheses. *Key Eng Mater* 2001; 23: 1535–1538.

5. Zeng P. *Biocompatible alumina ceramic for total hip replacements*. 2008. Epub ahead of print 2008. DOI: 10.1179/174328408X287682.

6. Jiang L, Liao Y, Wan Q, et al. Effects of sintering temperature and particle size on the translucency of zirconium dioxide dental ceramic. *J Mater Sci Mater Med* 2011; 22: 2429–2435.

7. Bearden LJ, Cooke FW. Growth inhibition of cultured fibroblasts by cobalt and nickel. *J Biomed Mater Res* 1980; 14: 289–309.

8. Gautam C, Joyner J, Gautam A, et al. Zirconia based dental ceramics: structure, mechanical properties, biocompatibility and applications. *Dalt Trans* 2016; 45: 19194–19215.

9. Bergman M, Bergman B, Söremark R. Tissue accumulation of nickel released due to electrochemical corrosion of non-precious dental casting alloys. *J Oral Rehabil* 1980; 7: 325–330.

10. Hayashi H, Saitou T, Maruyama N, et al. Thermal expansion coefficient of yttria stabilized zirconia for various yttria contents. *Solid State Ionics*. Epub ahead of print 2005. DOI: 10.1016/j.ssi.2004.08.021.

11. Lewis JA. Direct ink writing of 3D functional materials. *Adv Funct Mater* 2006; 16: 2193–2204.

12. Revelo CF, Colorado HA. 3D printing of kaolinite clay ceramics using the Direct Ink Writing (DIW) technique. *Ceram Int*. Epub ahead of print 2018. DOI: 10.1016/j.ceramint.2017.12.219.

13. Buj-Corral I, Domínguez-Fernández A, Gómez-Gejo A. Effect of printing parameters on dimensional error and surface roughness obtained in direct ink writing (DIW) processes. *Materials (Basel)*; 13. Epub ahead of print 2020. DOI: 10.3390/ma13092157.

14. Stanciuc AM, Sprecher CM, Adrien J, et al. Robocast zirconia-toughened alumina

scaffolds: Processing, structural characterisation and interaction with human primary osteoblasts. *J Eur Ceram Soc*. Epub ahead of print 2018. DOI: 10.1016/j.jeurceramsoc.2017.08.031.

15. Cesarano J, Dellinger JG, Saavedra MP, et al. Customization of load-bearing hydroxyapatite lattice scaffolds. *Int J Appl Ceram Technol* 2005; 2: 212–220.

16. Pieralli S, Kohal RJ, Jung RE, et al. Clinical Outcomes of Zirconia Dental Implants: A Systematic Review. *J Dent Res* 2017; 96: 38–46.

17. Pieralli S, Kohal RJ, Lopez Hernandez E, et al. Osseointegration of zirconia dental implants in animal investigations: A systematic review and meta-analysis. *Dent Mater* 2018; 34: 171–182.

18. Hodásová L, Sans J, Molina BG, et al. Polymer infiltrated ceramic networks with biocompatible adhesive and 3D-printed highly porous scaffolds. *Addit Manuf*; 39. Epub ahead of print 2021. DOI: 10.1016/j.addma.2021.101850.

19. Chen F, Zhu H, Wu JM, et al. Preparation and biological evaluation of ZrO2 all-ceramic teeth by DLP technology. *Ceram Int* 2020; 46: 11268–11274.

20. Shukla PP, Lawrence J, Wu H. Fracture toughness of a zirconia engineering ceramic and the effects thereon of surface processing with fibre laser radiation. *Proc Inst Mech Eng Part B J Eng Manuf*. Epub ahead of print 2010. DOI: 10.1243/09544054JEM1887.

21. Li M, Zhang L, Zhang C, et al. Effect of Y2O3 on the physical properties and biocompatibility of β–SiAlON ceramics. *Ceram Int* 2020; 46: 23427–23432.

22. Rashid H. The effect of surface roughness on ceramics used in dentistry: A review of literature. *European Journal of Dentistry*. Epub ahead of print 2014. DOI: 10.4103/1305-7456.143646.

23. Deltombe R, Kubiak KJ, Bigerelle M. How to select the most relevant 3D roughness parameters of a surface. *Scanning* 2014; 36: 150–160.

24. LLC MM. 3D S Parameters - Height (Amplitude) Parameters.

25. Sedlaček M, Gregorčič P, Podgornik B. Use of the Roughness Parameters S sk and S ku to Control Friction—A Method for Designing Surface Texturing. *Tribol Trans* 2017; 60: 260–266.

26. Oonishi H, Wakitani S, Murata N, et al. Clinical experience with ceramics in total hip

replacement. In: *Clinical Orthopaedics and Related Research*. 2000, pp. 77–84.

27. ISO25178. *ISO, I. (2010). 25178-6 Geometrical product specifications (GPS)-Surface texture: Areal-Part 6: Classification of methods for measuring surface texture. Geneva, Switzerland.* 2010.

28. Sanz-Fraile H, Amoros S, Mendizabal I, et al. Silk-Reinforced Collagen Hydrogels with Raised Multiscale Stiffness for Mesenchymal Cells 3D Culture. *Tissue Eng - Part A* 2020; 26: 358–370.

29. Shao H, Zhao D, Lin T, et al. 3D gel-printing of zirconia ceramic parts. *Ceram Int* 2017; 43: 13938–13942.

30. Sykaras N, Iacopino AM, Marker VA, et al. Implant materials, designs, and surface topographies: their effect on osseointegration. A literature review. *Int J Oral Maxillofac Implants*; 15.

31. Buj-corral I, Vidal D, Tejo-otero A, et al. Characterization of 3D Printed Yttria-Stabilized Zirconia Parts for Use in Prostheses. 2021; 1–12.

32. Chen J, Chen C, Chen Z, et al. Collagen/heparin coating on titanium surface improves the biocompatibility of titanium applied as a blood-contacting biomaterial. *J Biomed Mater Res - Part A* 2010; 95 A: 341–349.

33. Guo Y, Su Y, Gu R, et al. Enhanced corrosion resistance and biocompatibility of biodegradable magnesium alloy modified by calcium phosphate/collagen coating. *Surf Coatings Technol*; 401. Epub ahead of print 2020. DOI: 10.1016/j.surfcoat.2020.126318.

34. Hou Y, Yu L, Xie W, et al. Surface Roughness and Substrate Stiffness Synergize to Drive Cellular Mechanoresponse. *Nano Lett* 2020; 20: 748–757.